

Multifractality in critical neural field dynamics

Merlin Dumeur,^{1,2,3} Sheng H. Wang,^{1,2,3,4} J. Matias Palva,^{3,4,5,*} and Philippe Ciuciu^{1,2,*}

¹CEA, DRF, Joliot, NeuroSpin, Paris-Saclay University

²Inria MIND team, Paris-Saclay University

³Department of Neuroscience and Biomedical Engineering, Aalto University

⁴Neuroscience Center, Helsinki Institute of Life Science, Helsinki University

⁵Centre for Cognitive Neuroimaging (CCNi), Institute of Neuroscience and Psychology, University of Glasgow

(Dated: December 7, 2023)

The brain criticality framework has largely considered brain dynamics to be monofractal even though experimental evidence suggests that the brain exhibits significant multifractality. To understand how multifractality may emerge in critical-like systems, we use a computational model for critical neural oscillations. We find that multifractality emerges near a synchronization phase transition. These findings show multifractality in temporal dynamics peaks at criticality in neural fields, providing a generative model for interpreting multifractality in brain recordings.

INTRODUCTION

While the scale invariance of critical systems in the thermodynamic equilibrium is well established [1], dynamic systems far from equilibrium and operating near a critical point also display scale invariance [2, 3]. In the brain, scale invariance is usually characterized by using avalanches [4] where both spatial and temporal scaling can be quantified, and by self-similarity analysis on brain oscillations and behavior [5, 6] when only temporal information is available.

For a time series, scale invariance can be expressed as the power-law scaling of the q -th moments of some multi-resolution quantity: $\langle |T_X(j, k)|^q \rangle_k \propto 2^{j\zeta(q)}$. Self-similarity is characterized by the generalized Hurst exponent H [7], which is measured from $q = 2$, corresponding to the power spectrum [8]. Whereas monofractal time series have a single parameter H determine the scaling of every moment: $\zeta(q) = qH$, it is possible for different statistical moments to exhibit different scaling exponents [9], as can be found in turbulence [10] and financial [11] time series. In this case, the application of multifractal analysis (MFA) is warranted [12] to fully characterize $\zeta(q)$. In the case of the brain, recent findings show that the self-similar infra-slow (0.01-1 Hz) fluctuations of brain activity and behavioral performance [6, 13–15], exhibit significant multifractality [16, 17].

The brain is a large system exhibiting complex patterns such as spontaneous oscillations [18], whose dynamics have been suggested to arise from the brain operating near a critical point of a phase transition far from equilibrium, [19, 20] between synchronous and asynchronous phases [?]. Neuroscience research has taken advantage of computational modeling to understand the mechanisms underlying the emergence of critical dynamics in brain-like systems [21]. Thus, under the brain criticality hypothesis, the self-similarity in brain recording time series is understood to originate from the critical nature of the brain.

Multifractal analysis naturally extends self-similarity

analysis, and thus the multifractal properties of neural time series are expected to be linked to brain criticality. The analysis of the temporal dynamics of brain criticality models has, however, largely remained constrained to measures of self-similarity such as DFA [22], without accounting for potential multifractality. Thus the relationship between multifractal scaling and brain criticality [23, 24] has remained speculative and with limited basis in theory or generative models.

Here we investigate the emergence of multifractal scaling behavior and its relationship with self-similarity by analyzing simulations of a field model of neuronal population activity, a 'neural mass model', which has a critical point in a transition between synchronous and asynchronous phases [25].

We report the scaling properties of fluctuations in both the envelope of the modeled oscillation, as well as in the low-frequency domain. The model displays scale invariance across a range of temporal scales and, importantly, a divergence of multifractal exponents near the critical point of the phase transition. Further, simulations show multifractality is a result of finite size effects and vanishes in the thermodynamic limit.

MODEL AND MULTIFRACTAL FORMALISM

Landau-Ginzburg theory for cortical dynamics

The model simulated is derived from the Landau-Ginzburg field theory applied to the Wilson-Cowan neural mass model, as first proposed in [25]:

$$\begin{cases} \dot{\rho} &= (R - a)\rho + b\rho_i^2 - \rho^3 + h + D\nabla^2\rho + \sigma\sqrt{\rho}\eta \\ \dot{R} &= \frac{1}{\tau_R}(\xi - R) - \frac{1}{\tau_D}R\rho \end{cases} \quad (1)$$

The activity ρ corresponds to the excitatory neural activity term in the Wilson-Cowan equations, of which the third-order Taylor expansion has been kept, revealing

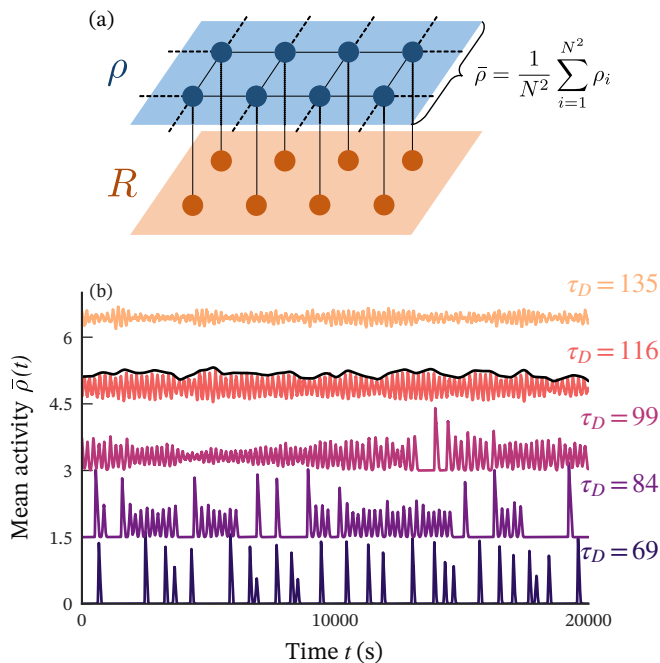


FIG. 1. Schema of the discretized model (a) in blue, the excitatory activity field ρ ; in orange the resource field R . Spatial average of the activity field (b) from simulations of the model, for varying values of the control parameter from subcritical to supercritical. Time series are each offset on the y-axis by 1.5 for legibility. The black line shows the oscillation envelope for one oscillatory signal.

the simplest formulation of a differential equation with a first-order phase transition. The “resources” term R represents inverse inhibitory neural activity. Since it evolves at a much slower time scale than ρ ($\tau_R \gg 1$, $\tau_D \gg 1$), it can be understood as the quasi self-organized control parameter of the excitatory field equation. Together, these coupled field equations reproduce the self-organized critical oscillation behavior [26], where neural oscillations emerge in a synchronisation phase transition, concurrently with power-law scaling avalanches. We investigate the phase transition by varying τ_D as our control parameter, which in the mean-field approximation controls the bifurcation from a limit cycle to bistable dynamics.

Figure 1 (b) showcases the transition from a down state ($\tau_D \leq 80$) with intermittent synchronous activity, to an up state containing oscillations ($\tau_D > 100$) displaying continuous asynchronous activity. In between the down phase and the critical point lies a bistable phase, where the dynamics of the Wilson-Cowan model alternate between synchronous spiking and asynchronous oscillations [27].

Simulations of the model were carried using a discrete version of the equations, approximating the fields with 2D square lattices, with edges of size N and toroidal boundary conditions (Figure 1 (a)).

Wavelet p -leader multifractal formalism

To determine the multifractal properties of the simulations, we look at the fluctuations in pointwise regularity as defined by the p -exponent [28]. We therefore necessarily rely on the corresponding wavelet p -leader formalism [29]. p -leaders are multi-resolution quantities which are derived from the wavelet transform $d_X(j, k)$ of a signal $X(t)$.

If we note $\lambda_{j,k} = [2^j k, 2^j(k+1))$ the dyadic interval associated with the temporal scale scale j and temporal shift k . Let $3\lambda_{j,k} = \lambda_{j,k-1} \cup \lambda_{j,k} \cup \lambda_{j,k+1}$ be the dyadic interval centered around $\lambda_{j,k}$ with three times the width.

The wavelet p -leaders are then defined as:

$$\ell_{j,k}^{(p)} := \left(\sum_{1 \leq j' \leq j} \sum_{k' \in 3\lambda_{j,k}} |d_X(j', k')|^p 2^{j-j'} \right)^{1/p}. \quad (2)$$

Given the wavelet p -leader description of a scale-invariant time series, the p -leader scaling function $\zeta^{(p)}(q)$ characterizes the scaling behaviour of its moments between the temporal scales $j_1 < j_2$:

$$\mathbb{E}_k \left[(\ell_{\lambda_{j,k}}^{(p)})^q \right] \propto 2^{j\zeta^{(p)}(q)}, \quad j \in [j_1, j_2].$$

Taking the Taylor expansion of $\zeta^{(p)}(q)$ around zero:

$$\zeta^{(p)}(q) = q c_1^{(p)} + \frac{q^2}{2} c_2^{(p)} + \frac{q^3}{6} c_3^{(p)} + \sum_{k=4}^{+\infty} \frac{q^k}{k!} c_k^{(p)}$$

where the p -leader log cumulants $(c_m^{(p)})_m$ are related to the moments of the multifractal spectrum: c_1 corresponds to the mode of the spectrum and measures self-similarity; c_2 corresponds to half of the width of the spectrum and measures multifractality. They are determined via linear regression from the cumulant scaling functions $C_m^{(p)}(j)$ over the scale interval $[j_1, j_2]$. These functions are defined as the m th-order cumulants of the log of the wavelet p -leaders, and scale as power laws with exponents $c_m^{(p)}$:

$$C_m^{(p)}(j) = \text{Cumulant}_m \left[\left(\log_2 \ell_{j,k}^{(p)} \right)_k \right] = j c_m^{(p)} + K_m.$$

A process is said multifractal if and only if $c_2^{(p)} < 0$. Otherwise, the signal is monofractal and all of its temporal scale-invariant properties are described by $c_1^{(p)}$. In this work, we restrict our analysis to the second order cumulants ($m \leq 2$), as it is the only order needed to showcase multifractality.

Hereafter $p = 2$ is fixed for comparability with results from Detrended Fluctuation Analysis (DFA); for the sake of clarity the (p) exponents are omitted from subsequent notations.

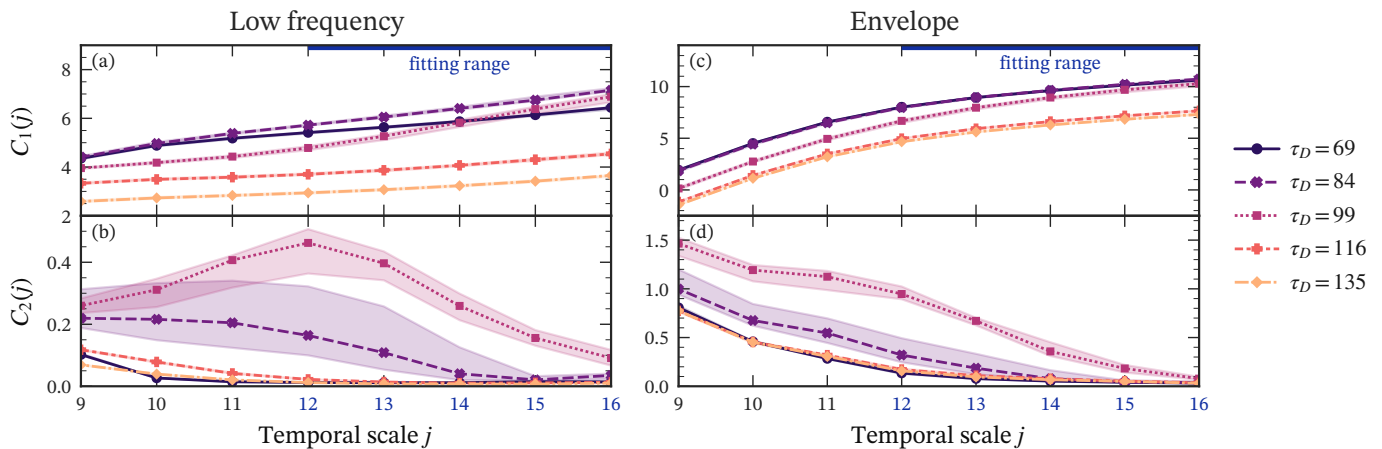


FIG. 2. Cumulant scaling functions $C_1(j)$ (top row) and $C_2(j)$ (bottom row) averaged over 20 simulations, for the low-frequency domain (a-b) and oscillation envelope (c-d), for five τ_D values introduced in Figure 1. Shaded area indicates 90% confidence interval over 20 simulations. In blue: range of scales $[j_1, j_2]$ over which the log-cumulants were estimated. The characteristic temporal scale of the oscillation is $j = 7.2$.

RESULTS

We simulated the model using the method proposed in [30] and improved in [31], implemented in python and GPU accelerated.

Except where specified, the simulation parameters were set to default values as follows: $\xi = 2.47, \tau_D = 100, \tau_R = 1000, a = 1, b = 1.5, h = 10^{-7}, D = \Delta_x = \sigma = 1, \Delta_t = 0.01, N = 128$. These correspond to the critical point of the phase transition investigated in [25]. Results are reported in the original time scale of the equation $1s = 100\Delta t$, where in our case the frequency associated to the scale j is $f_j = \frac{3}{4}2^{-j}$, hence these time scales evolve as the inverse of the log frequency. These units are arbitrary with regards to modeling brain activity, and could be adjusted to simulate physiological neural oscillations with any characteristic frequency, by simple scaling of the apparent sampling frequency.

The presence of a rare metastable steady state in the subcritical regime perturbs the proper estimation of the log-cumulants c_1 and c_2 in the low frequency case, and was addressed by removing segments of signal using a segmentation method described in the supplemental material (Supp. Figure 1).

The multifractal analysis was carried out using an implementation of the wavelet p -leader framework [32]. The analysis wavelet is the Daubechies wavelet with 3 vanishing moments. Wavelet p -leader based analysis has the additional requirement that the wavelet scaling function should be positive $\eta(p) > 0$. This is achieved by fractionally integrating the time series with coefficients $\gamma_{LF} = 1.5$, and $\gamma_{Env} = 1$, for the low frequency and envelope modalities respectively.

Scale invariance in the activity temporal trace

A necessary prerequisite for scale invariance analysis is the presence of scale invariance in the data. In order to meaningfully assess multifractality, we investigate the presence of scale invariance in the simulated time series, and fit our estimation of the log-cumulants in the range of temporal scales over which the time series are scale invariant. Under the wavelet p -leader formalism, scale-invariant time series have linear cumulant scaling functions $C_m(j)$.

The analysis is performed on the spatially coarse-grained excitatory activity process $\bar{\rho}(t) = \frac{1}{N^2} \sum_{i=1}^{N^2} \rho_i$. We report the scale invariance in the lower frequencies of the broadband signal, which is characteristic of critical dynamic models and which we term *low frequency*. The simulations are further filtered with a Morlet wavelet, which has for central frequency the characteristic frequency of the oscillations ($\omega_0 = 0.05\text{Hz}$), and shape parameter $\omega = 5$. The analysis results of the filtered data are reported as *envelope*.

Figure 2 shows cumulant scaling functions estimated from the simulations. The five simulations that are depicted illustrate how the model behaves in terms of scaling functions $(C_1(j), C_2(j))_j$ with varying τ_D . The $C_m(j)$ show a crossover at the scale $j = 12$, below which the scaling functions are dependent on characteristic effects from the evolution of the inhibitory field. Above that threshold, the scaling functions are linear which indicates scale invariance of the time series, thus the multifractal formalism is applicable.

We proceed with carrying out the multifractal analysis across the $j \in [12, 16]$ range for all simulations and for both modalities.

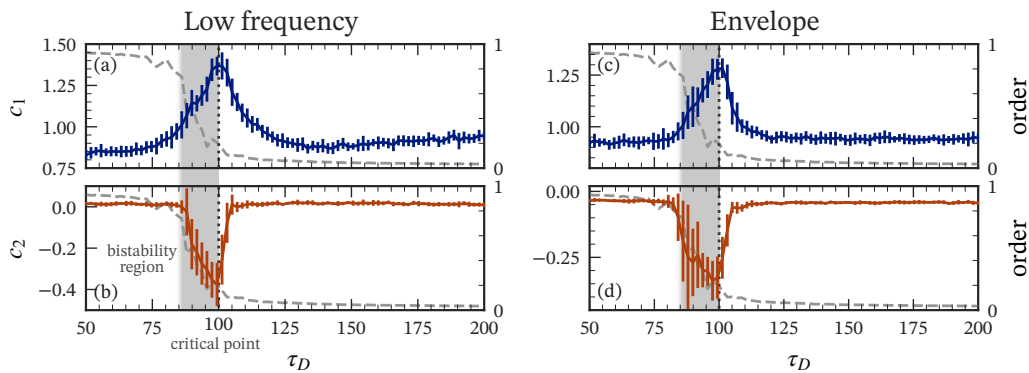


FIG. 3. Continuous lines: log-cumulants c_1 (top row) and c_2 (bottom row) across the phase transition for the low frequency domain (a-b) and the envelope (c-d). Error bars show the standard deviation over 20 simulations. Dashed grey lines show model order (Kuramoto synchronisation parameter K). Vertical dotted lines indicate the true critical point; the shaded area delimits the bistability region.

Multifractality near criticality

In order to assess the relationship between multifractality and the critical dynamics of the system, we now examine how the phase transition from the down state to the up state affects the log-cumulants $(c_m)_m$. Varying the resource depletion rate characteristic time scale τ_D , which controls the transition between limit cycle and bistable behaviour in the mean field approximation of the model, Figure 3 presents the c_m as a function of the control parameter: c_1 measures self-similarity and c_2 measures multifractality.

Relating the $(c_m)_m$ to the Kuramoto synchronization order parameter K shows that, in the low frequency regime, the $(c_m)_m$ take extremal values in a neighborhood of the critical point of the phase transition from order to disorder (dotted vertical line). Multifractality ($c_2 < 0$) is present in a neighborhood of the critical point and extends all the way through the bistable region (shaded area), but is absent from the rest of the parameter space ($c_2 = 0$).

Similarly for the oscillation envelope, the extremal values of the c_m fall on the critical point. However, in contrast to the low frequency case where $c_2 = 0$ far from the critical point, there is a constant minimal $c_2 < 0$ in the envelope estimates.

Fractional integration increases c_1 by the value of γ , and $\gamma_{LF} - \gamma_{Env} = 0.5$. Yet, the values of c_1 measured for the oscillation envelope are closer to the c_1 measured for the low frequency component than would be expected from fractional integration. Therefore, the oscillation envelope is overall a more regular time series than the low frequency component.

Finite size scaling

It has been shown [25] that in the thermodynamic limit, the asynchronous irregular (oscillatory) phase is confounded with the up state; and only the transition between the up state and the synchronous irregular (spiking) phase is present. Determining whether multifractality is present in the limit of large system sizes with constant coupling will show whether it is a true critical exponent or an effect of finite system sizes.

Figure 4 presents the resulting multifractal spectra obtained from simulations for increasing system sizes $N = 128, 256, 512$. We investigate the model in its multifractal regime for both low-frequency and envelope fluctuations, namely near the critical point.

While multifractality disappears in large N in the low frequency fluctuations, it remains in the oscillation envelope time series for the larger systems. Low frequency multifractality disappears together with the bistable state switching: the two phases of synchronous and asynchronous still exist in larger systems but the system alternates between those at a rate which diverges towards infinitely slow change as M increases.

On the other hand, the oscillation envelope stays multifractal in larger systems despite the increase stability of both phases. Analysis of the oscillation envelope considers fluctuations in the oscillation amplitude, which still occur in the larger system sizes. The measured spectra for the envelope get narrower as N increases, which is linked to the lower amplitude of the oscillations causing a lower dynamic range for the resulting oscillation envelope. Therefore, multifractality in the oscillation envelope is expected to decrease smoothly as a function of system size.

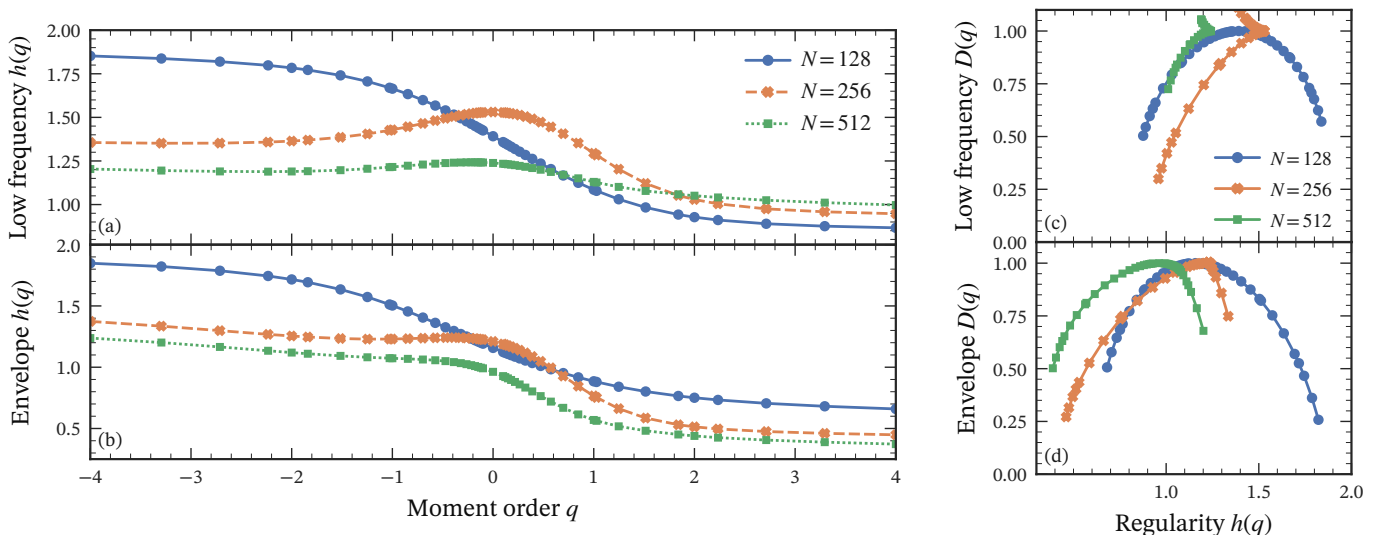


FIG. 4. Multifractal spectra for increasing system sizes. Regularity as a function of moment order, for (a) the low-frequency domain and (b) the oscillation envelope in the near-critical subcritical regime. (c-d) respectively corresponding multifractal spectra. The cusp-shaped spectra denote monofractal signals.

DISCUSSION

Low frequency vs envelope Both the low frequency fluctuations and oscillation envelope in the model display multifractality, which peaks at the critical point. This shows that they both behave as critical exponents to the same phase transition, even though they are measured on distinct elements of the time series. This finding validates the empirical use of the self-similarity of the oscillation envelope as relevant to determine criticality in brain recordings, and motivates using multifractal analysis on the oscillation envelope of neurophysiological recordings.

Neurophysiological relevance The presence of temporal multifractality in this model supports the empirical findings showing that multifractality is physiologically relevant either in the low-frequency-fluctuation case [17], or in the oscillation envelope [33]. In general, the intermittency of brain oscillatory processes has been outlined as physiologically relevant [34], but it remains transparent to characterizations strictly limited to self-similarity. In the context of brain criticality research, the results presented here motivate the use of multifractal analysis as a tool for understanding the organization of the brain's activity. The fact that self-similarity and multifractality are linked together to criticality in the model can be used as a starting point to formulate hypotheses about the dynamics of the brain, and which may be tested in order to check the validity of the modeling approach.

The results presented here may be readily extended to other neural field theories implementing self-organized critical oscillations [26], namely models having two coupled fields, with one showing a first-order phase transi-

tion (ρ), coupled to another slower evolving field which controls the phase transition (R). This represents an abstraction of brain activity which will require adjusting to real-life constraints and parameters, however the results will be expected to be qualitatively similar.

In conclusion, temporal multifractality emerges from self-organized critical oscillations theory, and gives a plausible explanation for the so far tentative link between self-organized brain criticality and empirical multifractality measured in cerebral time series.

This work is supported by the "ADI 2020" project funded by the IDEX Paris-Saclay, ANR-11-IDEX-0003-02 to M.D.; by ANR 19-CE48-0002-04 DARLING to M.D. and P.C.; by Sigrid Juselius Foundation to M.D., S.W. (210527), and J.M.P.; by the Instrumentarium Foundation to M.D.; and by the Finnish Cultural Foundation postdoc fellowship (00220071) to S.W.

* J.M.P. and P.C. contributed equally to this work

- [1] M. Kardar, *Statistical Physics of Fields* (Cambridge University Press, 2007).
- [2] M. Henkel and M. Pleimling, *Non-Equilibrium Phase Transitions* (Springer Netherlands, 2010).
- [3] U. C. Täuber, Phase transitions and scaling in systems far from equilibrium, *The Annual Review of Condensed Matter Physics* is **8**, 185 (2017).
- [4] J. M. Beggs and D. Plenz, Neuronal avalanches in neocortical circuits, *Journal of Neuroscience* **23**, 11167 (2003).
- [5] K. Linkenkaer-Hansen, V. V. Nikouline, J. M. Palva, and R. J. Ilmoniemi, Long-range temporal correlations and scaling behavior in human brain oscillations, *The Journal of Neuroscience* **21**, 1370 (2001).
- [6] J. M. Palva, A. Zhigalov, J. Hirvonen, O. Korhonen,

- K. Linkenkaer-Hansen, and S. Palva, Neuronal long-range temporal correlations and avalanche dynamics are correlated with behavioral scaling laws, *Proceedings of the National Academy of Sciences of the United States of America* **110**, 3585 (2013).
- [7] B. B. Mandelbrot and J. W. V. Ness, Fractional brownian motions, fractional noises and applications, *SIAM Review* **10**, 422 (1968).
- [8] C. Heneghan and G. McDarby, Establishing the relation between detrended fluctuation analysis and power spectral density analysis for stochastic processes, *Physical Review E* **62**, 6103 (2000).
- [9] H. E. Stanley and P. Meakin, Multifractal phenomena in physics and chemistry, *Nature* **335**, 405 (1988).
- [10] C. Meneveau and K. R. Sreenivasan, The multifractal nature of turbulent energy dissipation, *Journal of Fluid Mechanics* **224**, 429 (1991).
- [11] B. B. Mandelbrot, A multifractal walk down wall street, **280**, 70 (1999).
- [12] S. Jaffard, On davenport expansions (2004) pp. 273–303.
- [13] S. Monto, S. Palva, J. Voipio, and J. M. Palva, Very slow eeg fluctuations predict the dynamics of stimulus detection and oscillation amplitudes in humans, *The Journal of Neuroscience* **28**, 8268 (2008).
- [14] B. J. He, Scale-free brain activity: Past, present, and future, *Trends in Cognitive Sciences* **18**, 480 (2014).
- [15] P. Ciuciu, P. Abry, and B. J. He, Interplay between functional connectivity and scale-free dynamics in intrinsic fmri networks, *NeuroImage* **95**, 248 (2014).
- [16] P. Ciuciu, G. Varoquaux, P. Abry, S. Sadaghiani, and A. Kleinschmidt, Scale-free and multifractal time dynamics of fmri signals during rest and task, *Frontiers in Physiology* **3**, 10.3389/fphys.2012.00186 (2012).
- [17] D. L. Rocca, N. Zilber, P. Abry, V. van Wassenhove, and P. Ciuciu, Self-similarity and multifractality in human brain activity: A wavelet-based analysis of scale-free brain dynamics, *Journal of Neuroscience Methods* **309**, 175 (2018).
- [18] G. Buzsáki, *Rhythms of the Brain* (Oxford University Press, 2006).
- [19] J. J. Wright, R. R. Kydd, and G. J. Lees, State-changes in the brain viewed as linear steady-states and non-linear transitions between steady-states, *Biological Cybernetics* **53**, 11 (1985).
- [20] M. Breakspear, J. A. Roberts, J. R. Terry, S. Rodrigues, N. Mahant, and P. A. Robinson, A unifying explanation of primary generalized seizures through nonlinear brain modeling and bifurcation analysis, *Cerebral Cortex* **16**, 1296 (2006).
- [21] V. Zimmern, Why brain criticality is clinically relevant: A scoping review, *Frontiers in Neural Circuits* **14**, 10.3389/fncir.2020.00054 (2020).
- [22] S. H. Wang, F. Siebenhühner, G. Arnulfo, V. Myrov, L. Nobili, M. Breakspear, S. Palva, and J. M. Palva, Critical-like brain dynamics in a continuum from second- to first-order phase transition, *The Journal of Neuroscience*, JN (2023).
- [23] N. Zilber, Erf and scale-free analyses of source-reconstructed meg brain signals during a multisensory learning paradigm (2014).
- [24] G. Alamian, T. Lajnef, A. Pascarella, J.-M. Lina, L. Knight, J. Walters, K. D. Singh, and K. Jerbi, Altered brain criticality in schizophrenia: New insights from magnetoencephalography, *Frontiers in Neural Circuits* **16**, 10.3389/fncir.2022.630621 (2022).
- [25] S. di Santo, P. Villegas, R. Burioni, and M. A. Muñoz, Landau–ginzburg theory of cortex dynamics: Scale-free avalanches emerge at the edge of synchronization, *Proceedings of the National Academy of Sciences* **115**, E1356 (2018).
- [26] V. Buendía, S. di Santo, J. A. Bonachela, and M. A. Muñoz, Feedback mechanisms for self-organization to the edge of a phase transition, *Frontiers in Physics* **8**, 10.3389/fphy.2020.00333 (2020).
- [27] H. A. Golpayegan and A. D. Candia, Bistability and criticality in the stochastic wilson-cowan model, *Physical Review E* **107**, 10.1103/PhysRevE.107.034404 (2023).
- [28] S. Jaffard and C. Mélot, Wavelet analysis of fractal boundaries. part 1: Local exponents, *Communications in Mathematical Physics* **258**, 513 (2005).
- [29] S. Jaffard, C. Melot, R. Leonarduzzi, H. Wendt, P. Abry, S. G. Roux, and M. E. Torres, P-exponent and p-leaders, part i: Negative pointwise regularity, *Physica A: Statistical Mechanics and its Applications* **448**, 300 (2016).
- [30] I. Dornic, H. Chaté, and M. A. Muñoz, Integration of langevin equations with multiplicative noise and the viability of field theories for absorbing phase transitions, *Physical Review Letters* **94**, 100601 (2005).
- [31] H. Weissmann, N. M. Shnerb, and D. A. Kessler, Simulation of spatial systems with demographic noise, *Physical Review E* **98**, 022131 (2018).
- [32] Made available at <https://github.com/neurospin/pymultifrac>.
- [33] V. Catrambone, R. Barbieri, H. Wendt, P. Abry, and G. Valenza, Functional brain–heart interplay extends to the multifractal domain, *Philosophical Transactions of the Royal Society A: Mathematical, Physical and Engineering Sciences* **379**, 10.1098/rsta.2020.0260 (2021).
- [34] S. R. Jones, When brain rhythms aren’t ‘rhythmic’: implication for their mechanisms and meaning, *Current Opinion in Neurobiology* **40**, 72 (2016).